Structural and Dielectric Properties of $0.7(BiGd_xFe_{1-x}O_3)$-$0.3(PbTiO_3)$ (x=0.05-0.20) Multiferroic Composites

Krishna Auromun[1], N. K. Mohanty[2], S K. Satpathy[3], A. K. Behera[4], P. Nayak[5], Banarji Behera[6]

Materials Research Laboratory, School of Physics, Sambalpur University, Jyoti Vihar, Burla - 768019, Odish, India

Abstract— **The composites, $0.7(BiGd_xFe_{1-x}O_3)$-$0.3(PbTiO_3)$ (x=0.0, 0.05, 0.10, 0.15 and 0.20), were synthesized by mixed oxide route. The structural property and surface morphology (microstructures, grain sizes etc.) were studied by using X-ray diffraction and scanning electron microscope respectively.The systems were more distorted with the rise in Gd concentration. The value of dielectric constant (at room temperature) increased about two times in comparison to $0.5(BiGd_xFe_{1-x}O_3)$-$0.5(PbTiO_3)$ at 1kHz.**

Keywords— **Composites, X-Ray Diffraction, Scanning Electron Microscope and Dielectric Properties**

I. INTRODUCTION

In the recent year, some oxides exhibiting multiferroic properties with both ferroelectricity and magnetism, have attracted great interest in research. Multiferroic materials also known as magnetoelectric (ME) or ferroelectromagnetic materials, which exhibit both magnetization and dielectric polarization in a single phase. Multiferroic materials have gained tremendous attention on account of their potential applications in various fields such as satellite communication, digital recording, sensor, multiple state memory element, thin film capacitor, non-volatile memory, optoelectronics, solar energy device, permanent magnet, transducers, resistive switching elements, information storage, spintronics etc [1-4]

Among the different multiferroic material the perovskite $BiFeO_3$ (BFO) is one of the most promising multiferroic materials which is detected first time as early as the 1960s [5,6]. Bismuth ferrite (BFO) is one of the most extensively studied single phase multiferroic material at room temperature with antiferromagnetic-paramagnetic transition temperature at T_N=640K and ferroelectric Curie point at T_C=1100 K [7]. The relatively high conductivity of BFO is believed to be due to the reduction of Fe^{3+} species to Fe^{2+}, which creats oxygen vacancies for charge compensation. Hence, the special attention has been focused on synthesis of BFO with some other perovskites (ABO_3) such as $PbTiO_3$, $BaTiO_3$, $SrTiO_3$ and $Pb(Fe,Nb)O_3$, $Pb(Ti,Zr)O_3$ and $PbZrO_3$ [8-12] in order to improve the multiferroic and other related properties.

Among the above ABO_3 compounds, $PbTiO_3$ is one of the ferroelectric perovskite system with Tc~490ºC [13] which shows piezolectric properties.Realising the importance of $BiFeO_3$-$PbTiO_3$, we have reported the structural, dielectric properties of $0.7(BiGd_xFe_{1-x}O_3)$-$0.3(PbTiO_3)$ (x=0.0, 0.05, 0.10, 0.15 and 0.20), multiferroic composites.

II. EXPERIMENTAL

The composites $0.7(BiGd_xFe_{1-x}O_3)$-$0.3(PbTiO_3)$ were prepared by the solid state reaction technique by mixing stoichiometrically weighted ingredients (Bi_2O_3, Fe_2O_3, Gd_2O_3, PbO and TiO_2) of the best phase purity for x = 0.0, 0.05, 0.15 and 0.20. The powders were mixed and ground in an agate mortar to homogenize the mixture for 1 and half an hour in air and for 1 h in alcohol. Then the mixed powders were calcined at 800^0C in air for 5 h using an alumina crucible. The powders might be re-calcined till the required compound was formed. The formation of the compounds were studied by the X-ray diffraction (XRD) technique with a powder diffractometer (Rigaku Ultima IV, Japan) using Cu$K_\square$ radiation (λ=1.5405Å) in a wide range of Bragg's angles 2θ ($20^o \leq \theta \leq 80^o$) with a scanning rate of 3°/minute, and 0.02^o/ step. Then these calcined powders were used to form pellets of 12mm diameter at pressure of 3.5×10^6 Pa. using hydraulic press. The pellets were sintered at 850^oC for 5 hour in air. The pellets were silver coated and heated up to 150^oC to form parallel plate capacitor like arrangement for the electrical measurements. Generally, the dielectric properties of the materials were measured using an impedance analyzer, LCR meter (HIOKI, Model-3532) in the frequency range of 10^2-10^6 Hz and temperature range 25^oC-450^oC.

III. RESULTS AND DISCUSSION

A. Structural / Microstructural characterization

Fig 1. shows the room temperature X-ray diffraction (XRD) patterns of $0.7(BiGd_xFe_{1-x}O_3)$-$0.3(PbTiO_3)$ (x = 0.0, 0.05, 0.10, 0.15 and 0.20).

The XRD pattern confirms that the samples are crystalline in nature, and the peaks are well matched with the reported one [14]. Moreover, there is slight shifting of peak positions towards right in doping case, which signifies the increment of angle θ and the decrement of *d* (inter-planer spacing) and (*hkl*) values. The shifting of the peak position towards higher degree may be due to the distortion of the doped compound. As per the earlier report [15], the composite having 70% BFO and 30% PT, shows morphotropic phase boundary (MPB) in which both the rhombohedral and tetragonal phases coexist [16]. An extra peak (with * mark) observed at about 27.68^o (Bragg's angle) may be due to the presence of gadolinium (Gd) concentration [17] or due to the unavoidable formation of secondary (impurity) phase like $Bi_{25}FeO_{40}$ and $Bi_2Fe_4O_9$ [18-20]. The XRD data have been refined with tetragonal (*P4mm*) as well as rhombohedral (*R3c*) symmetry by using standard computer program package "POWD" [21]) and the lattice parameters were listed in the Table 1. The observed lattice parameters slightly differ from the reported one [20]. Further, the crystallite size of the composites can be determined by using the Debye Scherrer's equation [22]

$$P = \frac{K\lambda}{\beta_{1/2}\cos\theta}$$

, where K = constant, related to the crystallite shape, estimated as 0.89, θ = angle of incidence (glancing angle) for a particular plane, λ =1.5405Å, P = crystallite size, and $\beta_{1/2}$ = peak width of the reflection at half intensity. The average crystallite size (P) of the composites are found to be varying between 15-18 nm.

Fig. 2 shows the SEM micrographs of $0.7(BiGd_xFe_{1-x}O_3)$-$0.3(PbTiO_3)$ (x = 0.0, 0.05, 0.10, 0.15 and 0.20). The images confirm that the grains are spherical and uniformly distributed on the surface of the samples. The average grain size of the composites increases with the increase in gadolinium (Gd) concentration. The grain sizes for the composites are 0.5, 0.92, 1.32, 1.43 and 2 μm for x = 0.0, 0.10, 0.15 and 0.20 respectively. This increase in grain size refers to decrease in number of grain boundaries as well as resistivity. Some porosity is also observed after the doping of gadolinium. It is observed that crystallite size (in nm range) is much more less than grain size (in little μm range). Therefore, grains are composed of number of crystallites.

B. Dielectric study

The dielectric property includes the dielectric constant and dielectric loss. The dielectric constant of a material is to measure its ability to store charge relative to vacuum and characteristics of material.

The dielectric loss (*tanδ*) determines the insulating/conducting characteristics of material and also measures the energy loss per cycle (usually in the form of heat) from the material. The study of the dielectric properties of the ceramic over a wide range of temperature and composition is the principal tool for understanding ferroelectricity in the ceramic materials. A study of dielectric loss and dielectric constant of a sample as a function of frequency and temperature helps to understand the various polarization mechanisms present in them. The dipoles tend to align along the direction of an applied field for an AC fields and be in phase with it. However, the interaction of a dipole with other dipoles in the medium prevents this. This leads to dielectric loss, which appears as heat. This energy loss is connected with the imaginary part of the dielectric constant ε_r. Hence, we represent permittivity as a complex magnitude $\varepsilon_r = \varepsilon_r' - j\varepsilon_r''$. Very often the loss is expressed in terms of a quantity called the loss tangent

$$\tan\delta = \frac{\varepsilon_r''}{\varepsilon_r'}$$

. The angle δ is the complement of the angle between the applied electric field and the resultant current vector. Also, $\tan\delta$ increases with increase in temperature. Losses in these materials are mainly due to structural in-homogeneity, domain wall movement (i.e., grain rotation) and polarization [23].

Fig. 3 shows the variation of dielectric constant (ε_r) and dielectric loss (tanδ) of $0.7(BiGd_xFe_{1-x}O_3)$ - $0.3(PbTiO_3)$ for (x = 0.0, 0.05, 0.10, 0.15 and 0.20) with frequency at room temperature. In ε_r vs. frequency, there is decrease in ε_r with the increase in frequency. Because, at low frequency all types of polarizations are present. With the increase in frequency polarizations vanish one by one and only electronic polarization contribute at very high frequency. Similar type of behaviour occurs with tanδ as ε_r Vs frequency. Fig. 4 shows the variation of dielectric constant (ε_r) and dielectric loss (tanδ) of $0.7(BiGd_xFe_{1-x}O_3)$-$0.3(PbTiO_3)$ for x = 0.0, 0.05, 0.10, 0.15 and 0.20 with temperature at 10 kHz. With the increase in temperature the dielectric constant increases up to a particular temperature and then decreases. The peaks observed in the system $0.7(BiFeO_3)$-$0.3(PbTiO_3)$ in between 300^oC-400^oC are said to be anomalies. However, the phase-transition T_c value is at 575^oC [24]. These may be the indication of structural phase transition of composites between rhombohedral and tetragonal phases [24]. Similar trends are also observed in tanδ.

The increase in $\tan\delta$ signifies the rise of conductivity with the increase in temperature of the composites. Fig. 5 shows the variation of dielectric constant (ε_r) $0.7(BiGd_xFe_{1-x}O_3)-0.3(PbTiO_3)$ (x = 0.0, 0.05, 0.10, 0.15 and 0.20) with gadolinium (Gd) concentration at room temperature. The dynamical increment in dielectric constant occurs for small Gd concentration value. At low concentration (for x=0.05) of Gd, it is argued that the Gd ions acquire random distribution in the sample. In this situation, it is expected that no two Gd ions come closer to occupy nearest-neighbour sites to initiate interaction between them as the concentration is low. Under this situation they act as impurity to the system and electrons scatters by these ions causes more resistance [25]. This phenomenon gives rise to more resistivity as well as more dielectric constant due to impurity scattering of electron. As the Gd concentration is increased in the system, it is expected that more Gd ions occupy the nearest-neighbour sites to initiate interaction among them. Then the system may experience two three higher impurity cluster in comparison to the distribution of isolated single impurity Gd ions. Moreover, these clusters have their own energy distributions in the system. Therefore, it can be explained that the clusters of Gd ions might correlate to produce new energy labels in the vicinity of valence band which reduces energy gap between conduction band and valence band. Hence, conductivity increases where as resistivity as well as dielectric constant decrease significantly. The room temperature dielectric constant value reaches a maximum (588) for the Gd content x = 0.05 at a frequency 1 kHz. With further increase in Gd concentration, the value of the dielectric constant decreases. As compared to the parent composite, the electrical polarization as well as dielectric constant increases with further doping of Gd ion for x>0.10. This is due to the fact that the further doping of Gd^{3+} (0.938 Å) instead of Fe^{3+} (0.645 Å) increases the radii of B-site which gives rise to more distortion. Further, Fig. 5 confirms the inversely proportional behaviour of ε_r with frequency. Fig. 6 shows the variation of dielectric loss ($\tan\delta$) of $0.7(BiGd_xFe_{1-x}O_3)-0.3(PbTiO_3)$ (x = 0.0, 0.05, 0.10, 0.15 and 0.20) with gadolinium concentration at room temperature. The behaviour resembles with the dielectric constant as presented in Fig. 5.

TABLE I

Contents	Rhombohedral (R3c)*	Tetragonal (P4mm)*
$0.7(BiFeO_3)-0.3(PbTiO_3)$	a = 5.5991 Å c = 13.8188 Å	a = 3.9600Å c = 3.9772Å
$0.7(BiGd_{0.05}Fe_{0.95}O_3)-0.3(PbTiO_3)$	a = 5.5924 Å c = 13.7934 Å	a = 3.9592 Å c = 3.9656 Å
$0.7(BiGd_{0.10}Fe_{0.90}O_3)-0.3(PbTiO_3)$	a = 5.5715 Å c =13.7868 Å	a = 3.9387 Å c = 3.9478 Å
$0.7(BiGd_{0.15}Fe_{0.85}O_3)-0.3(PbTiO_3)$	a = 5.5726 Å c = 13.8023 Å	a = 3.9429 Å c = 3.9504 Å
$0.7(BiGd_{0.20}Fe_{0.80}O_3)-0.3(PbTiO_3)$	a =5.5693 Å c =13.7779 Å	a =3.9364 Å c =3.9445 Å
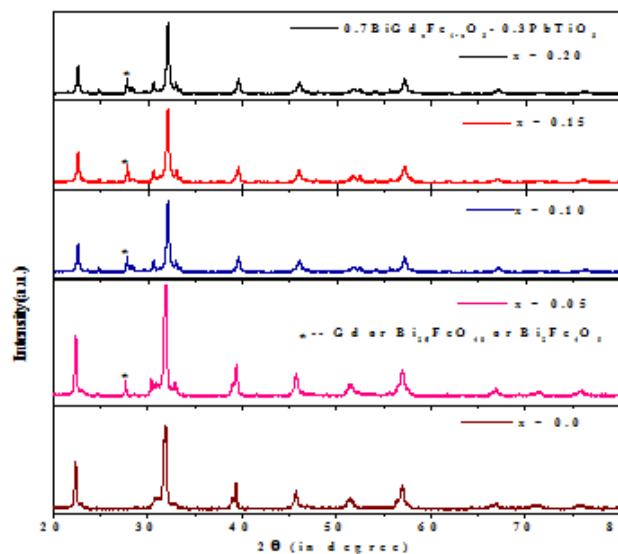
FIG.1
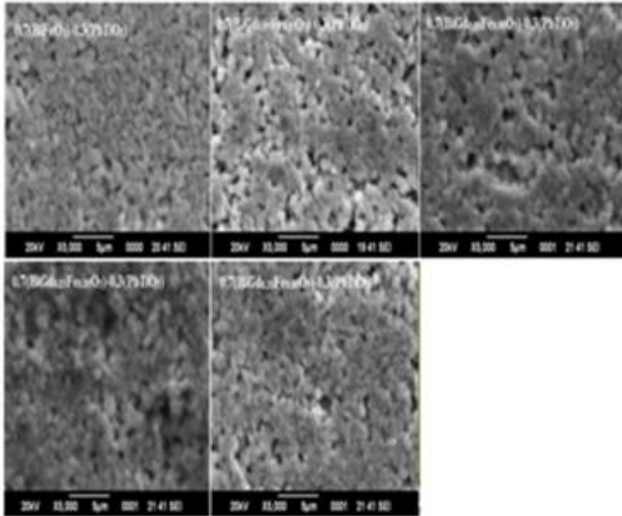
FIG.2
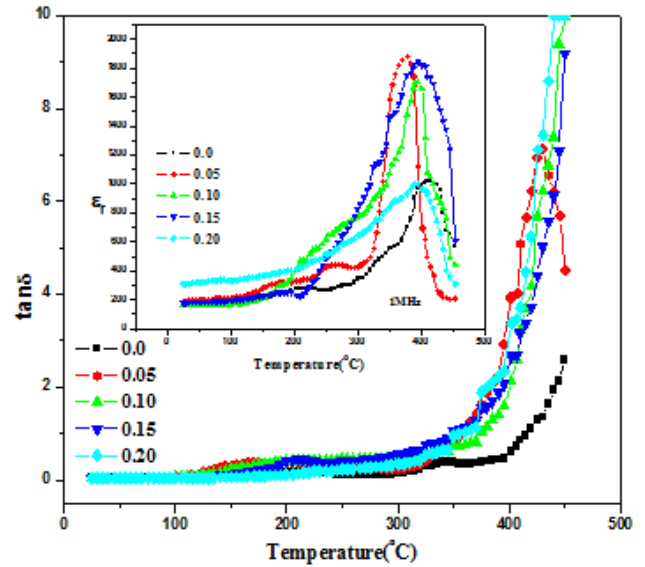
FIG.4
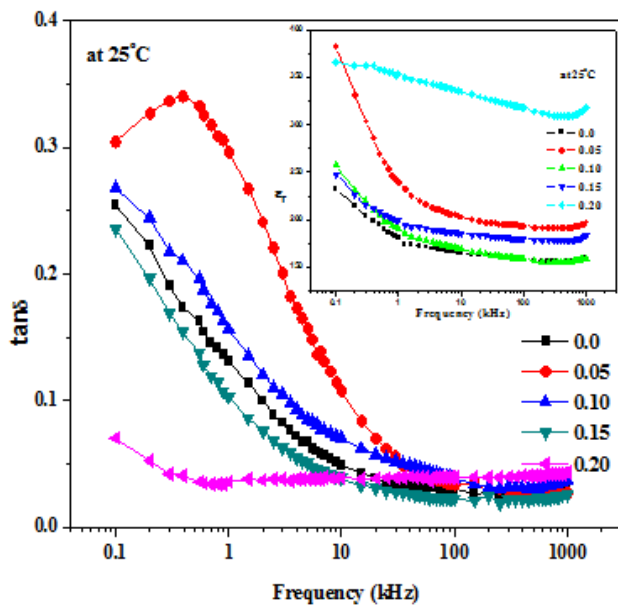
FIG.3
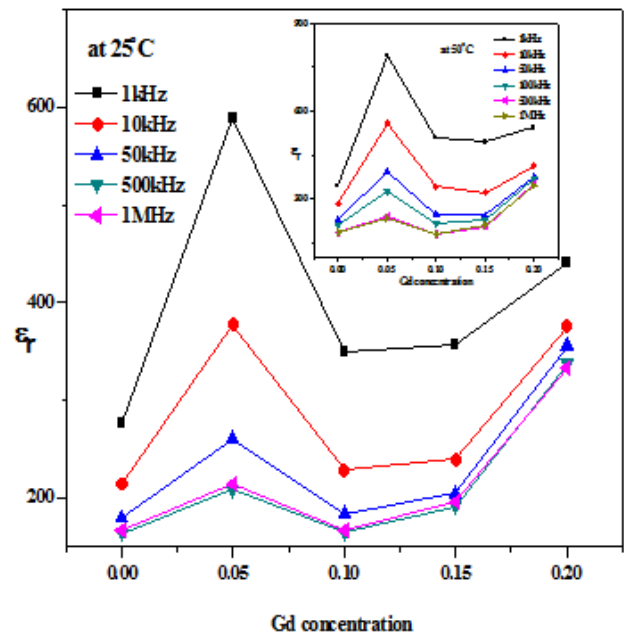
FIG.5
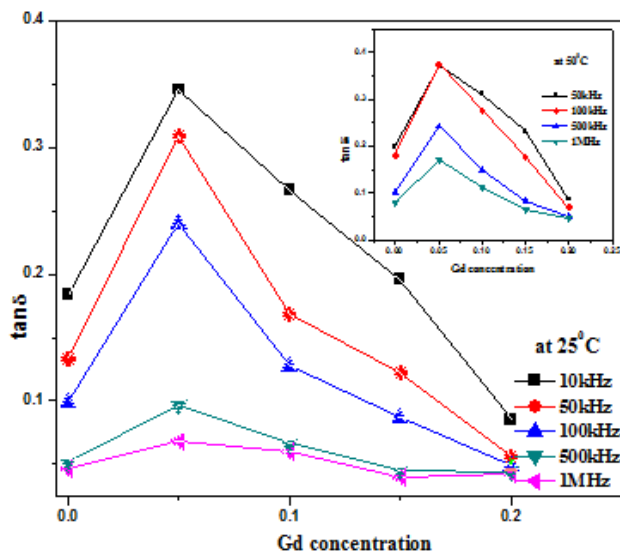
FIG.6

IV. CONCLUSION

The studied compounds $0.7(BiGd_xFe_{1-x}O_3)$-$0.3(PbTiO_3)$ show morphotropic phase boundary (MPB) in which both the rhombohedral and tetragonal phases coexist. Distortion occurs in the lattice structure of the samples after the doping of Gd. The complicated dielectric behavior is observed when the concentration of Gd is increased. The dynamical increment in dielectric constant occurs for small value of Gd concentration. The value of dielectric constant reaches maximum (588) at the Gd content $x = 0.05$. The crystallite size (in nm range), calculated from Scherrer's equation, is much more less than grain size (in µm range) observed from SEM. The grains are supposed to be composed of number of crystallites.

Figure Captions

Fig. 1 XRD patterns of $0.7(BiGd_xFe_{1-x}O_3)$-$0.3(PbTiO_3)$ (x = 0.0, 0.05, 0.10, 0.15 and 0.20).

Fig. 2 SEM micrographs of the samples $0.7(BiGd_xFe_{1-x}O_3)$- $0.3(PbTiO_3)$ (x=0.0, 0.05, 0.10, 0.15, 0.20).

Fig. 3 Variation of dielectric constant (ε_r) and dielectric loss (tanδ) of $0.7(BiGd_xFe_{1-x}O_3)$ - $0.3(PbTiO_3)$ (x=0.0, 0.05, 0.10, 0.15, 0.20) with frequency at room temperature.

Fig. 4 Variation of dielectric constant (ε_r) and dielectric loss (tanδ) of $0.7(BiGd_xFe_{1-x}O_3)$ - $0.3(PbTiO_3)$ (x=0.0, 0.05, 0.10, 0.15, 0.20) with temperature at 10 kHz.

Fig. 5 Variation of dielectric constant (ε_r) of $0.7(BiGd_xFe_{1-x}O_3)$ - $0.3(PbTiO_3)$ (x = 0.0, 0.05, 0.10, 0.15 and 0.20) with rare earth gadolinium concentration at room temperature and at 50^0C (figure inset)

Fig. 6 Variation of dielectric loss (tanδ) of $0.7(BiGd_xFe_{1-x}O_3)$ - $0.3(PbTiO_3)$ (x = 0.0, 0.05, 0.10, 0.15 and 0.20) with Gd concentration at room temperature and at 50^0C (figure inset)

C. Table Captions

Table 1 Refined lattice parameters of the samples of the system $0.7(BiGd_xFe_{1-x}O_3)$-$0.3(PbTiO_3)$ (x = 0.0, 0.05, 0.10, 0.15 and 0.20)

REFERENCES

[1] Qin W, Guo YP, Guo B, Gu M, *et al*. Dielectric and optical properties of BiFeO₃-(Na₀.₅Bi₀.₅)TiO₃ thin films deposited on Si substrate using LaNiO₃ as buffer layer for photovoltaic devices. *Alloys Compound* 2012, **513**: 154–158.

[2] Shami MY, Awan MS, Anis-Ur-Rehman M, Phase pure synthesis of BiFeO₃ nanopowders using diverse precursor via co-precipitation method. *J. Alloys Compd* 2011, **509**: 10139–10144.

[3] Chu YH, Martin LW, Holcomb MB, *et al*. Electric-field control of local ferromagnetism using a magnetoelectric multiferroic. *Nature Mater* 2008, **7**: 478-482.

[4] Rovillain P, De Sousa R, Gallais Y, *et al*. Electric-field control of spin waves at room temperature in multiferroic BiFeO₃. *Nature Mater* 2010, **9**: 975-979.

[5] Smolenskii GA, Agranovskaya AI, Dielectric Polarization and losses of some complex compounds. *Sov. Phys Tech Phys* 1958, **3:** 1380-1389.

[6] Smolenskii, G. A., Agranovskaya, A. I., Popov S. N., and Isupov, V. A. New ferroelectrics of complex composition. Sov Phys Tech Phys 1958, **28**: 2152.

[7] Catalan G, Scott JF, Physics and applications of Bismuth Ferrite. *Adv Mater* 2009, **21**: 2463-2485.

[8] Kumar M M, Srinivas A, Suryanarayana S V, Bhimasankaram T, Dielectric and impedance studies on BiFeO3- BaTiO3 solid solutions. *Phys. Status Solidi A.* 1998, **165**: 317.

[9] Kanai T, Ohkoshi S, Nakajima A, Watanabe T, Hashimoto K, A ferroelectric ferromagnet composed of (PLZT)*x* (BiFeO3)1−*x* solid solution. *Adv. Mater.* 2001, 13(7): 487.

[10] Ivanova T L, Gagulin V V, Dielectric properties in the microwave range of solid solutions in the BiFeO3-SrTiO3 system. *Ferroelectrics.* 2002, **265**: 241.

[11] Smith R T, Achenbach G D, Gerson R, James W J, Dielectric properties of solid solutions of BiFeO3 with Pb(Ti, Zr)O3 at high temperature and high frequency. *J. Appl. Phys.*, 1968, **39**: 70.

[12] Satpathy S K, Mohanty N K, Behera A K, Behera B, Nayak P, Electrical conductivity of Gd doped $BiFeO_3$- $PbZrO_3$ composite. *Front. Mater. Sci.,* 2013, **7**: 295.

[13] Jaffe B, Cook J W R., Jaffe H, Piezoelectric Ceramics. , vol. 7, pp 107, Journal of Sound and Vibration. 1971, **20**(4): 562.

[14] Comyn T P, McBride S P et al., *Materials Letters.* Processing and electrical properties of $BiFeO_3$–$PbTiO_3$ ceramics. 2004, **68**: 3844.

[15] Correas C, Hungria T et al., Mechanosynthesis of the whole (x) BiFeO3–(1-x) PbTiO3 multiferroic system: structural characterization and study of phase transitions. *J. Mater. Chem.,* 2011, **21**, 3125.

[16] Basith M A, Kurni O, et al., *Journal of Applied Physics.* Room temperature dielectric and magnetic properties of Gd and Ti co-doped $BiFeO_3$ ceramics. 2014, **115**: 024102.

[17] Mohanty N K, et al., Influence of Gd on structural and impedance properties of multiferroic composites: $BiFeO_3$-$PbTiO_3$. *Advanced Materials Letters*. 2015, **6**: 947.

[18] Kumar M, et al., Study of room temperature magnetoelectric coupling in Ti substituted bismuth ferrite system. *J. Appl. Phys.,* 2006, **100**: 074111.

[19] Xu J, Wang G, et al., Synthesis and weak ferromagnetism of Dy-doped BiFeO3 powders. *Mater. Lett.,* 2009, **63**: 855

[20] Karimi S, Reaney I M, et al., Nd-doped BiFeO 3 ceramics with antipolar order, *Applied Physics Letters.* 2009, **94**: 112903.

[21] Wu E: POWD, an interactive powder diffraction data interpretation and indexing program, Ver. 2.1, School of Physical Sciences, Flinders University South Bedford Park, SA 5042 Australia.

[22] Patterson A L. The Scherrer Formula for X-Ray Particle Size Determination. *Phys. Rev*., 1939, **56**: 978.

[23] Srivastava C M, and Srinivasan C, Science of Engineering Materials, Wiley Eastern Ltd., New Delhi 343 (1987).

[24] Correas C, Hungr T, et al., Mechanosynthesis of the whole xBiFeO3–(1 x)PbTiO3 multiferroic system: structural characterization and study of phase transitions. *J. Mater. Chem.,* 2011, **21**: 3125.

[25] Ashcroft N W, Mermin N D, Solid State Physics, Cengage Learning, Delhi 216 (1976).